ELSEVIER

Solar Energy Materials & Solar Cells 61 (2000) 19–33

Solar Energy Materials & Solar Cells

www.elsevier.com/locate/solmat

Photoinduced FT-IR spectroscopy and CW-photocurrent measurements of conjugated polymers and fullerenes blended into a conventional polymer matrix

C.J. Brabec[a,*], H. Johannson[a], F. Padinger[a], H. Neugebauer[a], J.C. Hummelen[b], N.S. Sariciftci[a]

[a]*Christian Doppler Laboratory for Plastic Solar Cells, Physical Chemistry, Johannes Kepler University of Linz, Altenbergerstr. 69, A-4040 Linz, Austria*

[b]*Stratingh Institute and Materials Science Center, University of Groningen, Nijenborgh 4, 9747 AG Groningen, Netherlands*

Abstract

In this work we present an investigation of the photoexcited states in conjugated polymer (donor) – fullerene (acceptor) interpenetrating networks embedded into conventional polymer hosts like polystyrene (PS), polyvinylcarbazole (PVK) or polyvinylbenzylchloride (PVBC) (guest – host approach), using photoinduced FT-IR spectroscopy. We discuss the influence of the specific host polymer matrices on the photoexcited states of the photoactive guests and investigate the photoinduced electron transfer by analysis of the infrared activated vibrational (IRAV) bands of poly-3-octylthiophene (P3OT) in comparative studies. Solar cells based on mixtures of poly [2-methoxy, 5-(3',7'-dimethyl-octyloxy)]-p-phenylene vinylene (MDMO-PPV), a highly soluble fullerene derivative [6,6]-phenyl C_{61}-butyric acid methyl ester (PCBM) and a conventional polymer (PS, PVK or PVBC) are characterized. We studied the current–voltage characteristics of devices and determined the energy conversion and electron/photon conversion efficiencies.

Keywords: Conjugated polymers; Fullerenes; Photovoltaic; IRAV; Host–guest systems

* Corresponding author.
E-mail address: christoph.brabec@jk.uni-linz.ac.at (C.J. Brabec)

0927-0248/00/$ - see front matter
PII: S0927-0248(99)00093-8

1. Introduction

The characterization of C_{60} as an electron acceptor capable of accepting as many as six electrons [1] candidates it as an acceptor in blends with conjugated polymers, which are good photoexcited electron donors. A wide class of these conjugated polymers and oligomers shows a photoinduced electron transfer from the excited state of the conjugated polymer onto a buckminsterfullerene, C_{60} [2,3]. The excellent acceptor properties of C_{60} together with the structural reorganization along the conjugated polymer backbone stabilize the photoinduced charge separated state. The electron transfer to C_{60} takes place on a timescale of less than one picosecond [4] and quenches strongly the photoluminescence as well as the intersystem crossing of the conjugated polymer in these composites. Obviously this process is efficiently competing with the dipole-allowed radiative emission as well as other non-radiative channels. The high quantum efficiency of the photoinduced charge transfer (close to unity) in conjugated polymer/fullerene blends candidates these composites as photoactive layers in solar cells.

The photoinduced charge transfer process is influenced by a number of factors. Generally, the ionization potential of the excited state of the donor (I_{D^*}), the electron affinity of the C_{60} (A_{C60}) and the Coulomb attraction of the separated radicals (U_C) including the polarization effects should match the following inequality:

$$I_{D^*} - A_{C60} - U_C \leqslant 0. \tag{1}$$

Eq. (1) is an essential but not sufficient condition for the charge transfer process, which may be influenced by other facts [5]. For instance, a potential barrier preventing the separation of the photoexcited electron–hole pair or the morphology of the blend preventing the overlap of the donor and acceptor excited state wave functions due to too large intermolecular spacing inhibit energetically allowed charge transfer processes.

Recently, increasing emphasis in research of conjugated polymers is placed on the engineering and processing of conjugated polymers in blends and composites with conventional polymers [6–9]. For these blends popular conventional polymers with excellent optical and mechanical properties like polystyrene (PS), polyethylene (PE), polyvinylcarbazole (PVK) or polyvinylbenzylchloride (PVBC) are used as host matrices. The guest – host approach is a sound method to improve the sample quality to enable the investigation of quasi one-dimensional systems for the following reasons:

(1) In thin films of these blends the highly diluted conjugated polymer, which may be compared to solid solutions, shows less interchain interaction compared to pure films.
(2) Macroscopic ordering and orientation of the conjugated polymer can be performed by mechanical uniaxial stretching of the guest polymer.
(3) In polymer blends the conjugated polymers are encapsulated in a highly stable host polymer, which protects the conjugated polymer against environmental influences.

Recent investigations showed that PE as a host matrix for conjugated polymer/fullerene devices has severe disadvantages compared to PS [10], like scattering or phase separation with fullerenes. The studies presented in this work are concentrated on three host matrices, each of them representing a characteristic property: PS because of its optical quality and its high compatibility with fullerenes and conjugated polymers, PVK because of the photoactivity of the carbazole sidegroup and PVBC because of its high dielectric constant.

2. Experimental

The chemical structure of the compounds investigated in this study is shown in Fig. 1. For the solar cells poly [2-methoxy, 5-(3',7'-dimethyl-octyloxy)]-p-phenylene vinylene [11] (MDMO-PPV) was used as the electron donor, while the electron acceptor was [6,6]-Phenyl C_{61}-butyric acid methyl ester [12] (PCBM). IRAV studies were carried out on poly-3-octylthiophene (P3OT) with C_{60} or PCBM as electron acceptor. The enhanced solubility of PCBM compared to C_{60} allows a high

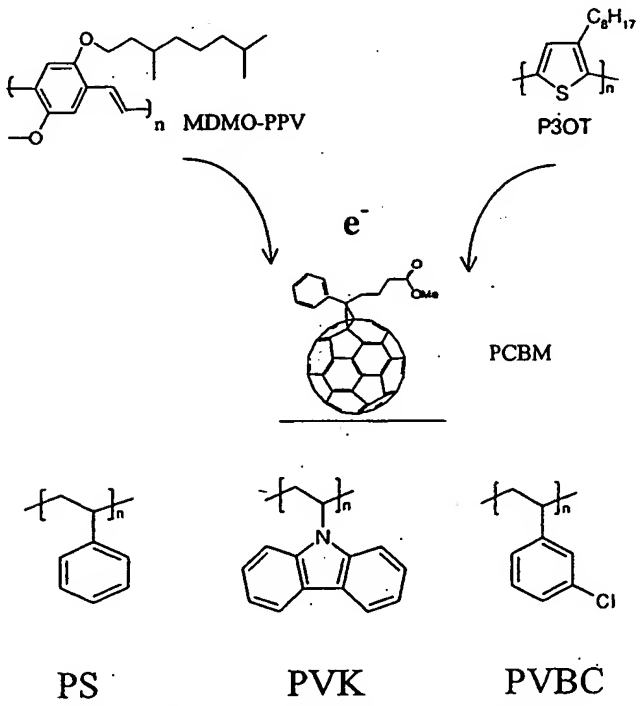

Fig. 1. Chemical structure of the investigated materials.

fullerene-conjugated polymer ratio and strongly supports the formation of donor–acceptor bulk heterojunctions. For the PS blends a Hostyren PS N 168 (Hoechst AG) was used while PVK and PVBC were received from Sigma Aldrich.

Photoinduced FTIR (PIA-FTIR) measurements were performed on composites with equal weight ratios of conventional polymer–P3OT–PCBM (1 : 1 : 1). Also C_{60} was used instead of PCBM in some experiments and for comparison the excited states of conventional polymer–P3OT composites without an electron acceptor were recorded. These samples were prepared from approximately 1 wt% solutions in 1,2-dichlorobenzene (ODCB). Infrared activated vibrational (IRAV) spectra were recorded on a Bruker IFS 66S spectrometer with a liquid-nitrogen cooled MCT detector. The samples for these experiments were prepared by drop casting from polymer solution on KBr pellets. The vacuum during all measurements was better than 10^{-5} Torr. The photo-induced charges in the infrared absorption spectra of the conjugated polymer were observed by measuring 10 single-beam spectra under illumination of the polymer sample and referencing them to 10 single-beam spectra taken in the dark. The samples were illuminated through a quartz window of the cryostat by an Ar^+ laser (488 nm, 20 mW/cm^2). For a better signal-to-noise ratio 200 repetitions of the measuring sequence described above were accumulated.

Photovoltaic devices were produced by spin casting from ODCB solution at ambient conditions. Optical quality films with high weight ratios of PCBM : alkoxy PPV are possible [13]. Solutions for spincasting were prepared with such concentrations, that the percentage of the MDMO-PPV is approximately 0.2–0.5 wt%. Depending on the concentration of the conjugated polymer moderate heating was necessary to prevent gelation. The weight ratio of the fullerene on the conjugated polymer was kept for all cells at 3 : 1 while the weight concentration of the conventional polymer was varied (0%, 11%, 20%, 33%, 50%, 66% and 80%). The typical film thickness of spincast films on ITO glass was around 80–150 nm. The non-transparent aluminum top electrode was evaporated thermally. The devices were mounted in a liquid-nitrogen bath cryostat and evacuated to 10^{-5} mbar. Photocurrents were measured under illumination on the ITO side through the quartz window of the cryostat by either a defocused Ar^+ laser beam at 488 nm or for the spectrally resolved measurements by a Xe arc lamp with a Czerny–Turner single-pass monochromator. The illumination intensity was kept constant at 1 mW/cm^2 at each wavelength in the range between 400 and 700 nm. Light intensities were measured by a calibrated Si photodiode. *I/V* curves were recorded by a Keithley 2400 Source Meter, typically by averaging 200 measurements for one point.

3. Results and discussion

3.1. Results from PIA FTIR spectroscopy

Fig. 2 shows that the photoinduced absorption spectra of P3OT changed considerably upon mixing an electron acceptor into the composite. Upon addition of a comparatively high weight fraction (1 : 1 ratio) of PCBM into the polymer compound,

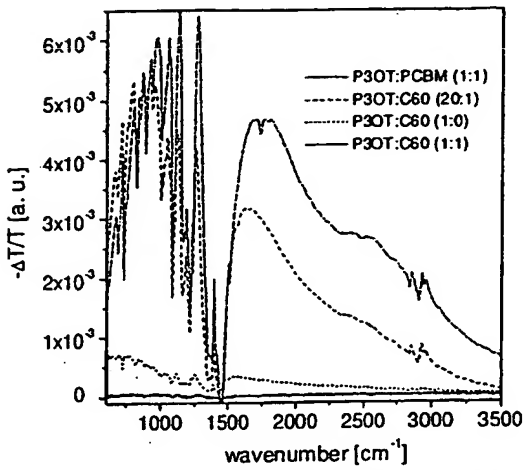

Fig. 2. PIA-FTIR spectrum of P3OT (· · ·) and P3OT with different fullerenes: P3OT: PCBM = 1 : 1) (– · – · –), P3OT : C_{60} = 1 : 1 (———) and P3OT : C_{60} = 20 : 1) (– – –). Samples were excited by an Ar^+ laser with 20 mW/cm² at 488 nm.

a bulk heterojunction donor–acceptor network is formed. The infrared activity of the P3OT/PCBM composite is enhanced by at least a factor of five without shifting the energetic positions of the photoinduced absorption peaks compared to pristine P3OT. The enhanced IRAV intensities of the conjugated polymer are interpreted by the subpicosecond photoinduced electron transfer from the conjugated polymer to the fullerene. This process governs a sufficient suppression of recombination, which increases the lifetime of the photogenerated charges and quenches all other competitive radiative and non-radiative relaxation processes. Both mechanisms yield an increased number of long living charged polarons, which are responsible for the observed enhancement of the infrared absorption signals.

A peculiar observation shown in Fig. 2 is that composites with a lower concentration of C_{60} (~ 5 wt%) in the conjugated polymer/fullerene network yield higher IRAV intensity than composites with a high concentration (~ 50 wt%). Microscope studies showed, that the morphology of a P3OT/PCBM composite allows donors and acceptors in the network to interact more closely compared to C_{60}. The differences in solubility of C_{60} compared to PCBM in the polymer network leads to phase separation and enhanced clustering. Enhanced clustering of a two component network at higher mixing ratios is a well-known phenomenon explained by the Flory theory for polymer solutions [14] and might explain the lower IRAV intensity of the P3OT/C_{60} (1 : 1) composite compared to the P3OT/C_{60} (20 : 1) composite.

Fig. 3 shows the IRAV response of P3OT upon mixing with PVK or PS. Neither PVK nor PS contribute to the IRAV bands of these composites. Furthermore, the IRAV intensity of P3OT is not enhanced upon mixing with one of the conventional

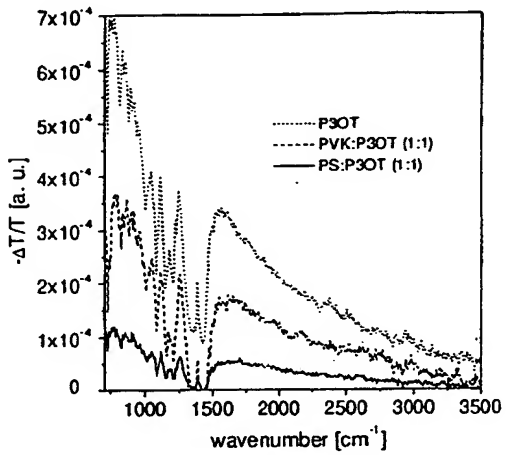

Fig. 3. PIA-FTIR spectrum of P3OT (· · ·) in different host matrices compared with PVK : P3OT = 1 : 1 (– – –) and PS : P3OT = 1 : 1 (———). Samples were excited by an Ar^+ laser with 20 mW/cm² at 488 nm.

polymers. It is therefore safe to conclude that both, PVK and PS do not show a photoinduced charge transfer with P3OT.

There is unambiguous evidence for a photoinduced charge transfer from one conventional polymer onto fullerene. As can be seen in Fig. 4 there is a weak but well defined photo-induced absorption for PVK with a peak at 4700 cm^{-1}. Pure PVK has an onset of absorption at around 300 nm while the pump energy for this experiment was 488 nm. Most likely a hole transfer from the photoexcited PCBM onto PVK [15] occurs. The photoactivity of PVK with PCBM opens the possibility to use PVK as an additional donor in photoinduced charge transfer heterojunctions.

Recent IRAV doping studies of P3OT [16,17] showed significant differences of the IRAV bands depending on the doping mechanism (i.e. chemical, electrochemical, photodoping). In the theoretical framework of the model presented by Zerbi et al. [18,19], the IRAV bands correspond to totally symmetric Raman active vibrational A_g modes, which couple to the π-electron system along a so-called "effective conjugation coordinate". The charge distribution in the formed polaronic or bipolaronic state causes high dipole moment changes during vibration, thereby breaking the symmetry. In general, in the frequency range between 1600 and 800 cm^{-1} four A_g modes exist in polythiophene, which, in unsubstituted polythiophenes, give rise to a pattern of three strong bands in the photoinduced absorption spectrum [20] and in the doping induced absorption spectrum [21] as well as to three main Raman bands. Very recently Ehrenfreund and Vardeny [22] established a link between the doping induced electronic state within the semiconducting π–π* energy gap and the IRAV bands of doping induced infrared spectra based on a linear response theory by Girlando et al. [23]. A clear coherence between the amount of doping and the position

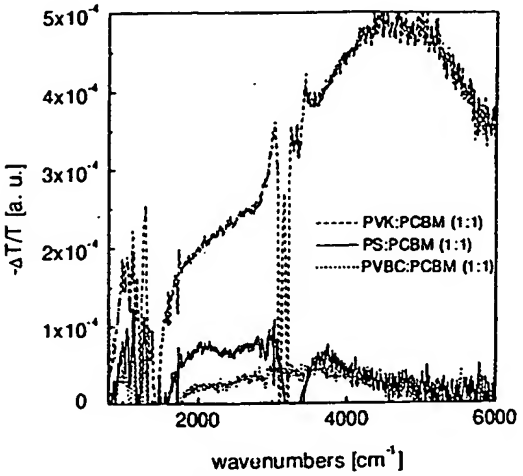

Fig. 4. PIA-FTIR spectrum of PCBM diluted in different conventional polymers: PVK : PCBM = 1 : 1 (– – –), PS : PCBM = 1 : 1 (———), PVBC : PCBM = 1 : 1 (· · ·).

of the IRAV bands and the electronic subgap absorption, respectively, was predicted. According to this analysis it was expected, that the IRAV features of a P3OT/PCBM composite should not change remarkably upon mixing into a conventional polymer. Fig. 5 shows PIA-FTIR spectra of different conventional polymer/P3OT/PCBM composites. No influence on the photoexcited states due to addition of the conventional polymer is observed. Even in the PVK/P3OT/PCBM composites, the IRAV activity of PVK as observed in PVK/PCBM composites is either absent or very weak compared to the photoinduced P3OT absorption bands.

3.2. *Results from photocurrent measurements*

A typical current–voltage characteristic of an ITO/MDMO-PPV–PCBM/Al photovoltaic device is compared with ITO/PVK–MDMO-PPV–PCBM/Al devices illuminated with 40 mW/cm² at 488 nm in Fig. 6a. Under these conditions the efficiency η_e calculates as $\sim 0.59\%$ with an I_{sc} of 2.13 mA/cm² and a V_{oc} of 0.72 V. Higher efficiencies are calculated at lower light intensities, where no photocurrent saturation occurs. Without external bias the PVK free device shows a short circuit current I_{sc} of up to 0.44 mA/cm² at 5 mW/cm² and an open circuit voltage V_{oc} of 720 mV. With a FF of 0.25 this gives a η_e of $\sim 1.6\%$. Addition of PVK does not alter the shape of the I/V curves but affects the absolute current values. No charge transfer complexes, as previously found for PVK and C_{60} composites [24], are detected in the investigated devices. The higher solubility and compatibility of PCBM with MDMO-PPV might be responsible for that. The same qualitative behavior was found for the other conventional polymers, i.e. PS and PVBC. Generally, the short-circuit

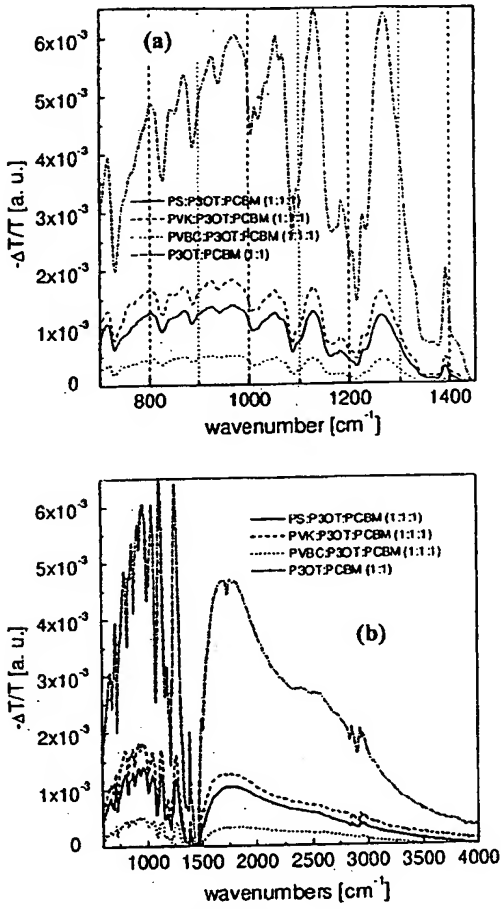

Fig. 5. PIA-FTIR spectrum of P3OT : PCBM = 1 : 1 (– · – · –) and upon dilution with the conventional polymers PS (———), PVK (– – –), PVBC (· · ·) at equal weight ratios in the range between 700 and 1500/cm (a) and in the full range (b).

currents I_{sc} but also the dark currents decreased with the addition of the conventional polymer to the pristine devices as can be seen from Fig. 6b. The decrease of the dark current upon increase of the conventional polymer concentration is ascribed to an ohmic contribution of the conventional polymer to the total serial resistance of the device.

Unexpectedly a high V_{oc} of 720 mV was observed in the pristine as well as in the guest–host photocells. In the metal–insulator–metal (MIM) diode picture the

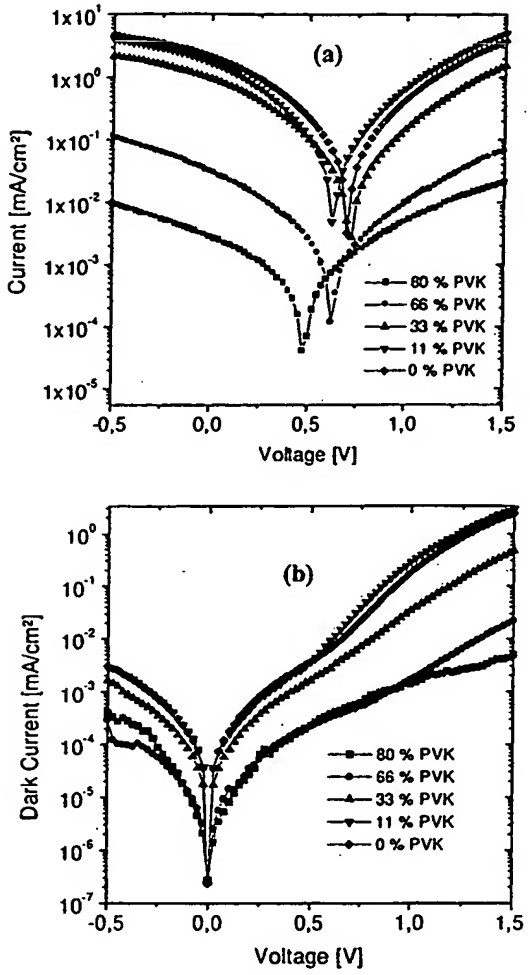

Fig. 6. (a) *I/V* curves of Al/PVK-MDMO-PPV-PCBM/ITO photocells. The concentration of the conventional polymer PVK in the blend is denoted in the figure. The devices were illuminated through the ITO side by 40 mW/cm² at 488 nm. (b) Dark *I/V* curves of Al/PVK-MDMO-PPV-PCBM/ITO photocells. The concentration of the conventional polymer PVK in the blend is denoted in the figure.

open-circuit voltage is generally accepted to arise from the work function difference of the two electrodes [25] which would yield a V_{oc} of 0.4 V (Al 4.3 eV; ITO 4.7 eV) or lower for interpenetrating network devices as observed by other groups [26,27]. In single-layer MEH-PPV devices sandwiched between ITO and Ca the V_{oc} was observed to follow the difference in the electrode work functions [28,29], consistent with

this model. Compared to pristine MEH-PPV photodiodes, addition of C_{60} lowers the average built in potential by 0.6 V, in accordance with the position of the C_{60}-LUMO level relatively to the MEH-PPV polaron level. Therefore, the MIM model cannot explain an open-circuit voltage as high as 0.72 V. The formation of space charge layers at the electrode/polymer interface [30] may lead to local potentials influencing the open-circuit potential. Capacitance measurements are in progress to investigate the occurrence of interfaces in interpenetrating network solar cells.

Between 60 and 80 wt% of PS a drop in the photocurrent is observed (Fig. 7). The same decrease of the photocurrent was measured in the PVK and PVBC blended photocells. Obviously one of the electroactive components reaches the percolation threshold. Small molecules like PCBM are expected to show a percolation threshold around a concentration of 17 vol% [31–33], while blends of conjugated polymers in conventional polymers have a much lower percolation threshold [34]. Therefore, it is expected that the disconnection of the percolated PCBM network paths is responsible for the photocurrent decrease above 80% conventional polymer content.

The total power conversion efficiency η_e of the cells under different illumination intensities was calculated using the relation

$$\eta_e = (V_{oc}(V) I_{sc}(\mathrm{A/cm^2}) \mathrm{FF}) / (P_{in}(W/\mathrm{cm^2}), \quad (2)$$

where V_{oc}, I_{sc}, FF, P_{in} are the open-circuit potential, short-circuit current, filling factor and incident light power, respectively. The filling factor was determined by calculation of the maximum power rectangular area under the I/V curve in the fourth quadrant. The filling factor FF was calculated by Eq. (3)

$$\mathrm{FF} = V_p I_p / (V_{oc} I_{sc}) \quad (3)$$

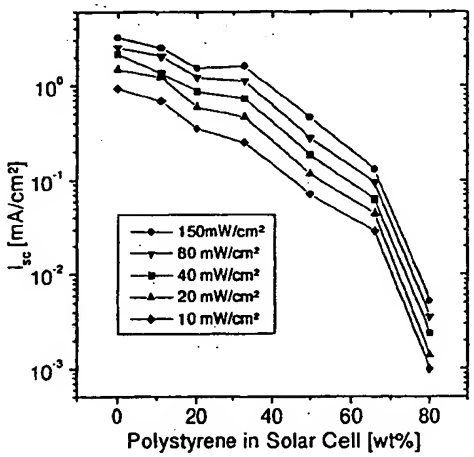

Fig. 7. Photocurrent of Al/PS–MDMO-PPV–PCBM/ITO devices at different illumination intensities (Ar^+ Laser, 488 nm) versus the PS concentration. The illumination densities are denoted inside the figure.

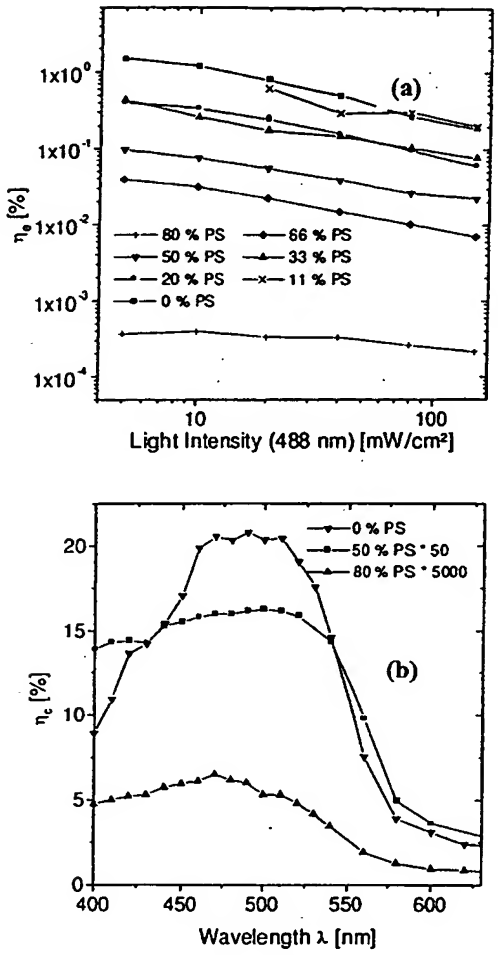

Fig. 8. (a) Power efficiency η_e of Al/PS–MDMO–PPV–PCBM/ITO devices versus excitation intensity. The devices were illuminated through the ITO glass. (b) Internal photon to carrier conversion efficiency η_c of Al/PS–MDMO–PPV–PCBM/ITO devices versus excitation wavelength. The devices were illuminated through the ITO glass with 1 mW/cm^2. η_c of the 50% and 80% PS device were multiplied by a factor 50 and 5000, respectively.

with V_p and I_p as the intersection of the I/V curve with the maximum power rectangle. With a FF of 0.25 a power efficiency of 1.6% under 5 mW/cm^2 of monochromatic light at 488 nm was calculated for the conventional polymer free devices. The pristine device shows a constant V_{oc} of 720 mV down to 5 mW/cm^2 irradiation intensity. The efficiency η_e of the cells decreased steadily with higher conventional

polymer concentrations (Figs. 8a, 9b and 10b). The spectrally resolved incident photon to converted electron efficiency (IPCE) η_e,

$$\eta_e(\%) = 1240 I_{sc}[\mu A/cm^2]/\lambda[nm]I[W/m^2], \tag{4}$$

calculated from the spectrally resolved short-circuit current values, is plotted in Figs. 8b, 9b and 10b for some selected host–guest devices. In Eq. (4) I and λ denote the

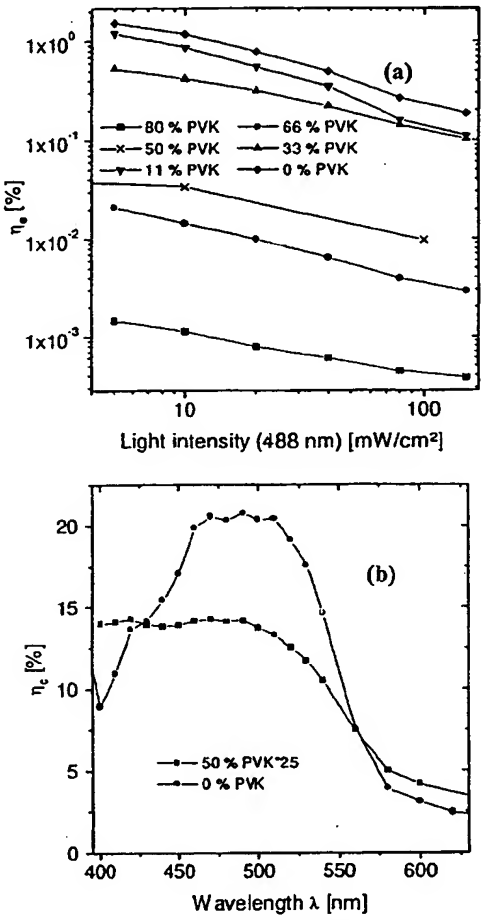

Fig. 9. (a) Power efficiency η_e of Al/PVK–MDMO-PPV–PCBM/ITO devices versus excitation intensity. The devices were illuminated through the ITO glass. (b) Internal photon to carrier conversion efficiency η_e of Al/PVK–MDMO-PPV–PCBM/ITO devices versus excitation wavelength. The devices were illuminated through the ITO glass with 1 mW/cm^2. η_e of the 50% PVK device was multiplied by a factor 25.

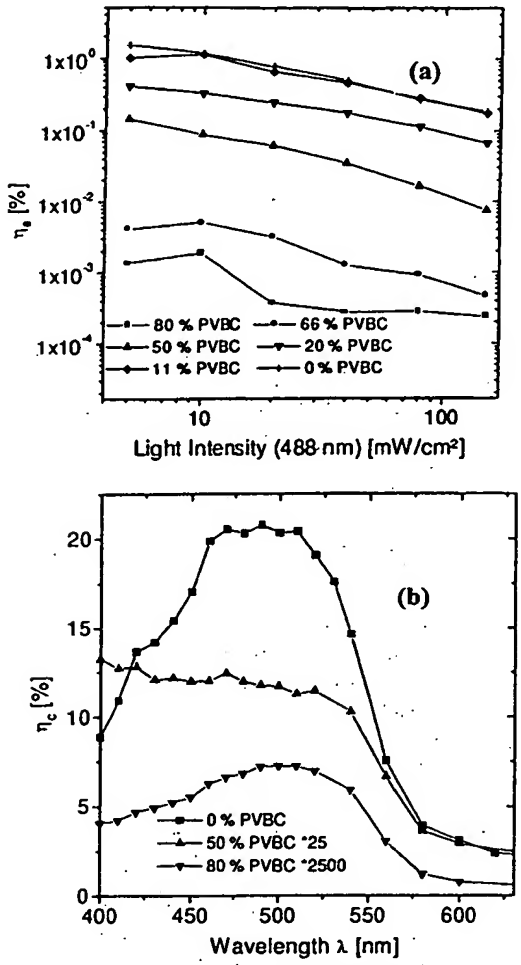

Fig. 10. (a) Power efficiency η_e of Al/PVBC–MDMO-PPV–PCBM/ITO devices versus excitation intensity. The devices were illuminated through the ITO glass. (b) Internal photon to carrier conversion efficiency η_c of Al/PVBC–MDMO-PPV–PCBM/ITO devices versus excitation wavelength. The devices were illuminated through the ITO glass with 1 mW/cm^2. η_c of the 50% and 80% PVBC device were multiplied by a factor 25 and 2500, respectively.

incident light intensity and the wavelength, respectively. The highest values of η_c ($\sim$ 20%) are again observed for the guest free device at the absorption maximum of the MDMO-PPV. Generally, the spectral photocurrent follows the absorption of MDMO-PPV with a very small contribution in the red spectral region. No filtering effects as found in pristine polymer photocells [35] were discovered in the guest–host

photocells, indicating balanced charge transport properties of the interpenetrating network.

The direct comparison of the power efficiency and the photon to carrier conversion efficiency of MDMO-PPV–PCBM devices diluted with different conventional polymers favors the use of PVK or PS over PVBC. The advantage of PS versus PVK is its better solubility in conventional organic solvents and its high compatibility with fullerenes.

4. Conclusion

Addition of electron acceptors into the conjugated polymer matrix enhances the photoinduced infrared absorption by at least one order of magnitude, but does not change the energetic positions of the IRAV bands or of the polaron sub-bandgap electronic absorption of P3OT. At 80 K P3OT/PCBM shows a stronger photoinduced IRAV response than a P3OT/C_{60} composite with similarly high fullerene concentration. Embedding of the photoactive charge transfer system into a conventional polymer host matrix does not shift the positions of the lower-energy infrared bands and the polaron absorption peak, respectively. PVK, which is a conventional polymer, can be used as additional electron donor for PCBM independent of conjugated polymers.

For large-scale production of plastic solar cells, the rheological properties as well as the environmental stability is highly relevant. Small amounts of PS, PVK or PVBC (10 wt%) did not change the efficiency of the cells significantly. Further increasing of the conventional polymer concentration results in a strong decrease of the I_{sc}. The percolation threshold for the interpenetrating network of the conjugated polymer/methanofullerene mixture in the host matrix determines the onset of enhanced photovoltaic response.

Acknowledgements

This work is performed within the Christian Doppler Foundations dedicated laboratory on Plastic Solar Cells funded by the Austrian Ministry of Economic Affairs and Quantum Solar Emergy Linz Ges. m. b. H. The work is further supported by the "Fonds zur Förderung der wissenschaftlichen Forschung" of Austria (Project No. P-12680-CHE) and the Netherlands Organization for Energy & Environment (NOVEM).

References

[1] P.M. Allemand, A. Koch, F. Wudl, Y. Rubin, F. Diederich, M.M. Alvarez, S.J. Anz, R.L. Whetten, J. Am. Chem. Soc. 113 (1991) 1050.
[2] N.S. Sariciftci, L. Smilowitz, A.J. Heeger, F. Wudl, Science 258 (1992) 1474.

[3] L. Smilowitz, N.S. Sariciftci, R. Wu, C. Gettinger, A.J. Heeger, F. Wudl, Phys. Rev. B 47 (1993) 13835.
[4] B. Kraabel, J.C. Hummelen, D. Vacar, D. Moses, N.S. Sariciftci, A.J. Heeger, F. Wudl, J. Chem. Phys. 104 (1996) 4267.
[5] R.A.J. Janssen, N.S. Sariciftci, A.J. Heeger, J. Chem. Phys. 100 (1994) 8641.
[6] S. Hotta, S.D.D.V. Rughooputh, A.J. Heeger, Synth. Met. 22 (1987) 79.
[7] J.S. Uhm, H.-W. Schmidt, Polym. Prep. Am. Chem. Soc. 34 (1993) 725.
[8] J. Moulton, P. Smith, J. Polym. Sci. 30 (1992) 871.
[9] T.W. Hagler, K. Pakbaz, A.J. Heeger, Phys. Rev. B 49 (1994) 10968.
[10] C.J. Brabec, V. Dyakonov, N.S. Sariciftci, W. Graupner, G. Leising, J.C. Hummelen, J. Chem. Phys. 109 (1998) 1185.
[11] G.H. Gelinck, J. Warman, E.G.J. Staring, J. Chem. Phys. 100 (1996) 5485.H. Spreitzer, W. Kreuder, H. Becker, H.F.M. Schoo, R. Demandt, PCT Patent Application WO 98/27136, 1996.
[12] J.C. Hummelen, B.W. Knight, F. Lepec, F. Wudl, J. Org. Chem. 60 (1995) 532.
[13] J. Gao, F. Hide, H. Wang, Synth. Met. 84 (1997) 979.
[14] P.J. Flory, Principles of Polymer Chemistry, Cornell University Press, Ithaca and London, 1953.
[15] Y. Wang, Nature 356 (1992) 585.
[16] H. Johannson, C.J. Brabec, H. Neugebauer, J.C. Hummelen, R.A.J. Janssen, N.S. Sariciftci, Synth. Met., in print.
[17] K. Lee, E.K. Miller, N.S. Sariciftci, J.C. Hummelen, F. Wudl, A. J Heeger, Phys. Rev. B 54 (1996) 10525.
[18] G. Zerbi, M. Gussoni, C. Castiglioni, in: J.L. Brédas, R. Silbey (Eds.), Conjugated Polymers, Kluwer, Dordecht, 1991, pp. 435–507.
[19] G. Zerbi, C. Castiglioni, M. Del Zoppo, in: K. Müllen, G. Wegner (Eds.), Electronic Materials: The Oligomer Approach, Wiley-VCH, New York, 1998, pp. 345–402.
[20] Z. Vardeny, E. Ehrenfreund, O. Brafman, A.J. Heeger, F. Wudl, Synth. Met. 18 (1987) 183.
[21] H. Neugebauer, A. Neckel, N. Brinda-Konopik, in: H. Kuzmany, M. Mehring, S. Roth (Eds.), Electronic Properties of Polymers and Related Compounds, Springer Series in Solid State Sciences, Vol. 63, Springer, Berlin, 1985, p. 227.
[22] E. Ehrenfreund, Z.V. Vardeny, J. Int. Opt. Eng. (SPIE) 3145 (1997) 324.
[23] A. Girlando, A. Painelli, Z.G. Soos, J. Chem. Phys. 98 (1993) 7459.
[24] Y. Wang, A. Suna, J. Phys. Chem. B 101 (1997) 5627.
[25] I.D. Parker, J. Appl. Phys. 75 (1993) 1656.
[26] L.S. Roman, M.R. Andersson, T. Yohannes, O. Inganäs, Adv. Mater. 9 (1997) 1164.
[27] K. Yoshino, K. Tada, M. Hirohata, H. Kajii, Y. Hironaka, N. Tada, Y. Kaneuchi, M. Yoshida, A. Fijii, M. Hamaguchi, H. Araki, T. Kawai, M. Ozaki, Y. Ohmori, M. Onoda, A.A. Zakhidov, Synth. Met. 84. (1997) 477.
[28] G. Yu, A.J. Heeger, J. Appl. Phys. 78 (1995) 4510.
[29] G. Yu, C. Zhang, A.J. Heeger, Appl. Phys. Lett. 64 (1994) 1540.
[30] W.R. Salaneck, S. Stafström, J.-L. Bredas, Conjugated Polymer Surfaces and Interfaces, Cambridge University Press, Cambridge, 1996.
[31] A. Aharony, D. Stauffer, Introduction to Percolation Theory, 2nd Edition, Taylor and Francis, 1993.
[32] A.J. Heeger, TRIP 3 (1995) 39.
[33] C.J. Brabec, F. Padinger, V. Dyakonov, J.C. Hummelen, R.A.J. Janssen, N.S. Sariciftci, in: H. Kuzmany, M. Mehring, S. Roth (Eds.), Molecular Nanostrucutures, Proceedings of the International Winterschool on Electronic Properties of Novel Materials, Kirchberg, 1998, pp. 519–522.
[34] A. Fizazi, J. Moulton, K. Pakbaz, S.D.D.V. Rughooputh, P. Smith, A.J. Heeger, Phys. Rev. Lett. 64 (1990) 2180.
[35] M. Granström, K. Petritsch, A.C. Aries, A. Lux, M.R. Andersson, R.H. Friend, Nature 395 (1998) 257.